

Verification of the Maxwell–Stefan theory for diffusion of three-component mixtures in zeolites

R. Krishna*, D. Paschek

Department of Chemical Engineering, University of Amsterdam, Nieuwe Achtergracht 166, 1018 WV Amsterdam, The Netherlands

Received 16 March 2001; accepted 29 May 2001

Abstract

We develop the Maxwell–Stefan formulation for diffusion of multicomponent mixtures in zeolites and show that the mixture transport behaviour can be predicted on the basis of information of the pure component jump diffusivities at zero loading. The interaction between the diffusing, sorbed, species is taken into account by introduction of an interchange coefficients \mathcal{D}_{ij} . The interchange coefficients \mathcal{D}_{ij} encapsulate the correlations in the molecular jumps. A logarithmic-interpolation formula is suggested for estimating these interchange coefficients from the information on the pure component jump diffusivities. To verify the developed Maxwell–Stefan formulation, we have carried out kinetic Monte Carlo (KMC) simulations to calculate the transport diffusivities for a ternary mixture in silicalite. The KMC simulations confirm that the ternary mixture diffusion can be predicted with good accuracy with the Maxwell–Stefan theory. © 2002 Elsevier Science B.V. All rights reserved.

Keywords: Maxwell–Stefan theory; Zeolites; Mixture diffusion; Kinetic Monte Carlo simulations; Correlation effects

1. Introduction

In the design of zeolite-based adsorption or catalytic processes, it is essential to have a proper description of diffusion of mixtures within the zeolite crystals [1–3]. For n -component diffusion, the fluxes \mathbf{N}_i are related to the gradients of the fractional occupancies $\nabla\theta_i$ by the following relation:

$$(\mathbf{N}) = -\rho[\Theta_{\text{sat}}][D](\nabla\theta) \quad (1)$$

where $[D]$ is the n -dimensional square matrix of Fick diffusivities, ρ the zeolite-matrix density expressed as unit cells per m^3 , $[\Theta_{\text{sat}}]$ a diagonal matrix with elements $\Theta_{i,\text{sat}}$, representing the saturation loading of species i . The fractional occupancies θ_i are defined as

$$\theta_i \equiv \frac{\Theta_i}{\Theta_{i,\text{sat}}}, \quad i = 1, 2, \dots, n \quad (2)$$

where Θ_i represents the loading of species i expressed in molecules of sorbate per unit cell.

For estimation of the fluxes \mathbf{N}_i , we need to estimate the $n \times n$ elements of $[D]$. The elements of $[D]$ are influenced not only by the species mobilities but also by the sorption thermodynamics [4]. For design purposes, it is important to have

a mixture diffusion theory with the capability of predicting the elements of $[D]$ from pure component transport data. Such mixture diffusion theories are almost invariably based on the theory of irreversible thermodynamics (IT) [4–7]. In the Onsager IT formulation, a linear relation is postulated between the fluxes and the chemical potential gradients:

$$(\mathbf{N}) = -\rho[\Theta_{\text{sat}}][L]\frac{1}{RT}\nabla(\mu) \quad (3)$$

where R is the gas constant, T the temperature, $\nabla(\mu)$ the column matrix of chemical potential gradients, $\nabla\mu_i$ represent the correct driving forces for diffusion, $[L]$ the square matrix of Onsager coefficients having the units $[\text{m}^2/\text{s}]$. The Onsager matrix $[L]$ is non-diagonal, in general, and the cross-coefficients portray the coupling between species diffusion. The Onsager reciprocal relations demand that the matrix $[L]$ be symmetric, i.e.

$$L_{ij} = L_{ji}, \quad i = 1, 2, \dots, n \quad (4)$$

The chemical potential gradients in Eq. (3) may be expressed in terms of the gradients of the occupancies by introduction of the matrix of thermodynamic factors $[\Gamma]$:

$$\frac{\theta_i}{RT}\nabla\mu_i = \sum_{j=1}^n \Gamma_{ij}\nabla\theta_j, \quad \Gamma_{ij} \equiv \left(\frac{\Theta_{j,\text{sat}}}{\Theta_{i,\text{sat}}}\right) \frac{\Theta_i}{p_i} \frac{\partial p_i}{\partial \Theta_j}, \quad (5)$$

$i, j = 1, 2, \dots, n$

* Corresponding author. Tel.: +31-20-525-7007; fax: +31-20-525-5604. E-mail address: krishna@its.chem.uva.nl (R. Krishna).

Nomenclature

$[B]$	square matrix of drag coefficients (m^2/s)
D	Fick, or transport, diffusivity of component 1 in zeolite (m^2/s)
$[D]$	matrix of Fick diffusivities (m^2/s)
\mathcal{D}_i	Maxwell–Stefan diffusivity of species i in zeolite (m^2/s)
\mathcal{D}_{ij}	Maxwell–Stefan diffusivity describing interchange between i and j (m^2/s)
D^*	tracer or self-diffusivity (m^2/s)
ℓ	displacement distance (m)
$[L]$	matrix of Onsager coefficients (m^2/s)
n	number of diffusing species, dimensionless
N	number of sorbed particles in KMC simulation, dimensionless
\mathbf{N}_i	molecular flux of species i (molecules/ $\text{m}^2 \text{ s}$)
p_i	jump probability for the i th process, dimensionless
P	system pressure (Pa)
\mathbf{r}	particle displacement vector (m)
R	gas constant ($8.314 \text{ J mol}^{-1} \text{ K}^{-1}$)
T	absolute temperature (K)

Greek letters

Γ	thermodynamic correction factor, dimensionless
$[\Gamma]$	matrix of thermodynamic factors, dimensionless
θ_i	fractional surface occupancy of component i
Θ_i	molecular loading (molecules per unit cell or per cage)
$\Theta_{i,\text{sat}}$	saturation loading (molecules per unit cell or per cage)
μ_i	molar chemical potential (J mol^{-1})
ν	jump frequency (s^{-1})
ρ	density of zeolite (number of unit cells/ m^3)

Subscripts

1, 2, 3	referring to species 1, 2 and 3
int	intersections
sat	referring to saturation conditions
str	straight channel
zz	zig-zag channel

Vector and matrix notation

()	column vector
[]	square matrix

Operators

∇	gradient or nabla
----------	-------------------

Knowledge of the sorption isotherm is sufficient to allow estimation of $[\Gamma]$ and $\nabla(\mu)$. If the n -component sorption can be described by the multicomponent Langmuir isotherm, the elements of $[\Gamma]$ are given by

$$\Gamma_{ij} = \delta_{ij} + \frac{\theta_i}{1 - \theta_1 - \theta_2 - \dots - \theta_n},$$

$$i, j = 1, 2, \dots, n \quad (6)$$

where δ_{ij} is the Kronecker delta.

Combining Eqs. (1), (5) and (6), we obtain

$$(\mathbf{N}) = -\rho[\Theta_{\text{sat}}][L] \begin{bmatrix} \frac{1}{\theta_1} & 0 & 0 \\ 0 & \ddots & 0 \\ 0 & 0 & \frac{1}{\theta_n} \end{bmatrix} [\Gamma](\nabla\theta) \quad (7)$$

Comparing Eqs. (1) and (7), we obtain the inter-relation:

$$[D] = [L] \begin{bmatrix} \frac{1}{\theta_1} & 0 & 0 \\ 0 & \ddots & 0 \\ 0 & 0 & \frac{1}{\theta_n} \end{bmatrix} [\Gamma] \quad (8)$$

The Fick matrix $[D]$ can be estimated from knowledge of the Onsager matrix $[L]$. Unfortunately, the IT theory provides no fundamental guidelines for estimating $[L]$ from data on pure component transport coefficients.

The objectives of the present communication are the following:

1. To develop a procedure for estimating $[L]$ and $[D]$ from pure component transport data; for this purpose we resort to the Maxwell–Stefan formulation.
2. To validate the Maxwell–Stefan theory for estimating $[L]$ and $[D]$ by performing KMC simulations for ternary diffusion in silicalite.

2. The Maxwell–Stefan theory of diffusion in zeolites

In the Maxwell–Stefan formulation, entirely consistent with the theory of IT, the chemical potential gradients are written as linear functions of the fluxes [4,7–9]:

$$-\rho \frac{\theta_i}{RT} \nabla \mu_i = \sum_{j=1, j \neq i}^n \frac{\Theta_j \mathbf{N}_i - \Theta_i \mathbf{N}_j}{\Theta_{i,\text{sat}} \Theta_{j,\text{sat}} \mathcal{D}_{ij}} + \frac{\mathbf{N}_i}{\Theta_{i,\text{sat}} \mathcal{D}_i},$$

$$i = 1, 2, \dots, n \quad (9)$$

We have to reckon in general with two types of Maxwell–Stefan diffusivities: \mathcal{D}_i and \mathcal{D}_{ij} . The \mathcal{D}_i are the diffusivities that reflect interactions between species i and the zeolite matrix; they are also referred to as jump or “corrected” diffusivities in the literature [3,4]. Mechanistically, the Maxwell–Stefan diffusivity \mathcal{D}_i may be related to the displacement of the adsorbed molecular species, ℓ , and the jump

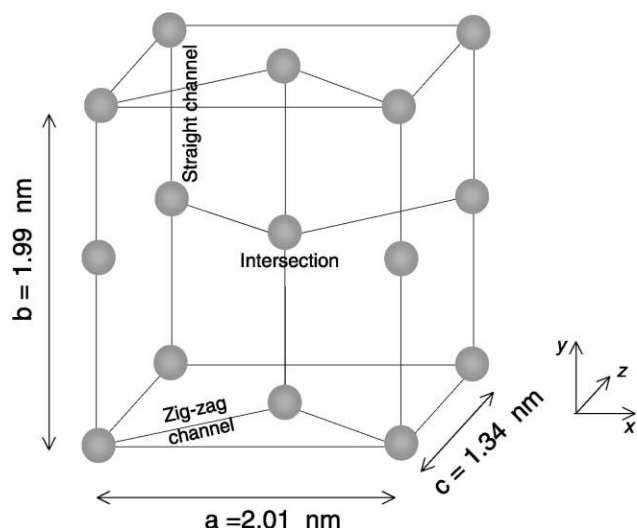


Fig. 1. Diffusion unit cells for silicalite. The large dots indicate the sorption sites, located at the intersections between the straight and zig-zag channels.

frequency, or transition probability, ν , which in general can be expected to be dependent on the total occupancy [10–13].

For the silicalite topology (see Fig. 1), Kärger [14] has derived the following set of relations:

$$\begin{aligned} \mathcal{D}_1(0) &= \frac{1}{3}(\mathcal{D}_x(0) + \mathcal{D}_y(0) + \mathcal{D}_z(0)), \\ \mathcal{D}_x(0) &= \frac{1}{4}v_{zz}a^2, \\ \mathcal{D}_y(0) &= \frac{1}{4}v_{\text{str}}b^2, \quad \mathcal{D}_z(0) = \frac{1}{4} \frac{v_{\text{str}}v_{zz}}{v_{zz} + v_{zz}}c^2 \end{aligned} \quad (10)$$

where v_{str} and v_{zz} are the jump frequencies for the movement along the straight (str) and zig-zag (zz) channels, respectively, and the dimensions a , b and c are as specified in Fig. 1. For specific molecules, the zero loading diffusivity $\mathcal{D}_i(0)$ can be determined experimentally or by use of transition state theory [2,15–19].

The jump frequency ν can be expected to decrease with occupancy [10–13]. If we assume that a molecule can migrate from one site to another only when the receiving site is vacant, the chance that this will occur will be a function of the fraction of unoccupied sites. A simple model for Maxwell–Stefan diffusivity is

$$\mathcal{D}_i = \mathcal{D}_i(0)(1 - \theta_1 - \theta_2 - \dots - \theta_n) \quad (11)$$

Additionally, molecular repulsive forces come into play when determining the jump frequency of molecules. Due to molecular repulsions, the jump frequency increases because a molecule wishes to escape from the “unfavourable” environment. Clearly, the molecular repulsions will increase when the occupancy increases [20]. The overall effect of repulsive interactions could be to ensure that the Maxwell–Stefan diffusivity \mathcal{D}_i is independent of occupancy, in conformity with a lot of experimental data [1–3].

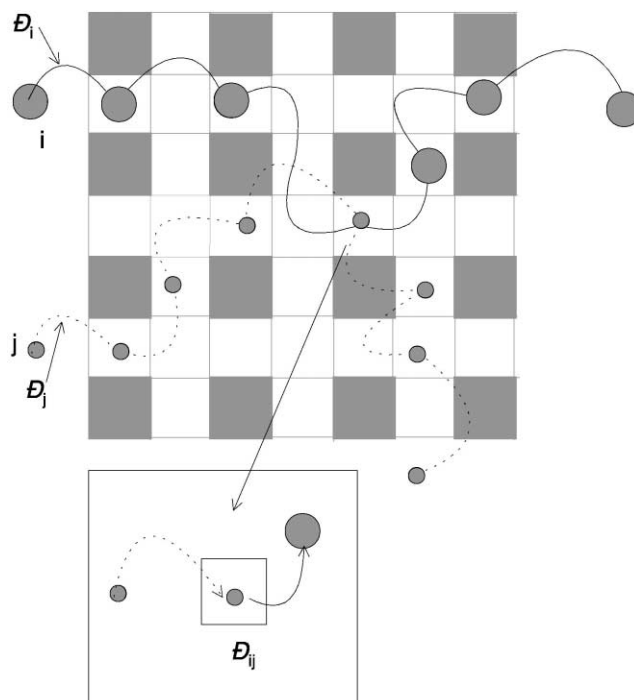


Fig. 2. Pictorial representation of the two types of diffusivities for binary mixtures using the Maxwell–Stefan model.

Mixture diffusion introduces an additional complication due to sorbate–sorbate interactions. This interaction is embodied in the coefficients \mathcal{D}_{ij} . We can consider this coefficient as representing the facility for counter-exchange, i.e. at a sorption site, the sorbed species j is replaced by the species i ; see Fig. 2. The Onsager reciprocal relations require $\mathcal{D}_{ij} = \mathcal{D}_{ji}$. The net effect of this counter-exchange is a slowing down of a faster moving species due to interactions with a species of lower mobility. Also, a species of lower mobility is accelerated by interactions with another species of higher mobility. As shown by Krishna and Paschek [20,21], \mathcal{D}_{ij} encapsulates the correlation effects associated with molecular jumps. The interchange coefficient \mathcal{D}_{ij} can be estimated by the logarithmic-interpolation formula that has been suggested by Krishna and Wesselingh [4]:

$$\mathcal{D}_{ij} = [\mathcal{D}_i]^{\theta_i/(\theta_i+\theta_j)} [\mathcal{D}_j]^{\theta_j/(\theta_i+\theta_j)} \quad (12)$$

It is convenient to define an n -dimensional square matrix $[B]$ with elements

$$\begin{aligned} B_{ii} &= \frac{1}{\mathcal{D}_i} + \sum_{j=1, j \neq i}^n \frac{\theta_j}{\mathcal{D}_{ij}}, \\ B_{ij} &= -\frac{\theta_i}{\mathcal{D}_{ij}}, \quad i, j = 1, 2, \dots, n \end{aligned} \quad (13)$$

With this definition of $[B]$, Eq. (9) can be cast into n -dimensional matrix form

$$(\mathbf{N}) = -\rho[\Theta_{\text{sat}}][B]^{-1}[\Gamma]\nabla(\theta) \quad (14)$$

which gives the following expressions for the Onsager and Fick matrices:

$$[L] = [B]^{-1} \begin{bmatrix} \theta_1 & 0 & 0 \\ 0 & \ddots & 0 \\ 0 & 0 & \theta_n \end{bmatrix}, \quad [D] = [B]^{-1}[I]. \quad (15)$$

For single component diffusion, Eq. (15) simplifies to

$$L_1 = \mathcal{D}_1 \theta_1, \quad D_1 = \frac{\mathcal{D}_1}{1 - \theta_1}. \quad (16)$$

For single component diffusion, Eq. (16) shows that none of the three coefficients, Fick, Maxwell–Stefan and Onsager, are influenced by correlation effects [20]. The situation changes when we consider mixtures of two or more species. Eq. (15) shows that the interchange coefficients \mathcal{D}_{ij} , portraying correlated molecular jumps, will influence *all* the elements of $[L]$ and $[D]$. In another way, the main elements of the Onsager matrix L_{ii} cannot be identified with pure component coefficients, as has been erroneously suggested in the literature by Sundaram and Yang [6].

In order to verify Eqs. (12), (13) and (15) for estimation of $[L]$ and $[D]$, we perform KMC simulations for ternary mixture diffusion in silicalite.

3. KMC simulation methodology

We perform KMC simulations for a three-component mixture in which each component follows Langmuir isotherm behaviour. We assume the lattice to be made up of equal-sized sites which can be occupied by only one molecule at a time and there are no further molecule–molecule interactions such as repulsive forces. Particles can move from one site to a neighbouring site via hops. For silicalite, the jump frequencies along the straight and zig-zag channels for component 2 are taken to correspond to that for 2-methyl hexane (2MH) at 300 K, $\nu_{1,\text{str}} = 1.4 \times 10^5/\text{s}$, $\nu_{1,\text{zz}} = 5 \times 10^4/\text{s}$, these values were calculated by Smit et al. [15] using the transition state theory. The maximum loading was taken to be 4 molecules per unit cell, where the molecules are all located at the intersections. We have published the details of the pure component 2MH simulations earlier [22,23]; these simulations have established the validity of Eq. (11) to describe the variation of the jump diffusivity \mathcal{D}_i with occupancy. The jump frequencies for components 1 and 3 are taken to be, respectively, half and twice, the corresponding values for component 2. Table 1

Table 1
Transition probabilities and zero-loading diffusivities for three component

Species, i	$\Theta_{1,\text{sat}}$	$\nu_{\text{zz}} (\text{s}^{-1})$	$\nu_{\text{str}} (\text{s}^{-1})$	$\mathcal{D}_i (0) (\text{m}^2/\text{s})$
1	4	2.5×10^4	7×10^4	3.43×10^{-14}
2 (=2MH)	4	5×10^4	1.4×10^5	6.86×10^{-14}
3	4	1×10^5	2.8×10^5	13.72×10^{-14}

summarises the jump frequencies and the zero-loading jump diffusivities for all the three components.

We employ a standard KMC methodology to propagate the system (details in Refs. [21–25]). A hop is made at every KMC step and the system clock is updated with variable time steps. For a given configuration of random walkers on the lattice, a process list containing all the possible M moves to vacant intersection sites is created. Each possible move i is associated with a transition probability ν_i . Now, the mean elapsed time τ is the inverse of the total rate coefficient

$$\tau^{-1} = \nu_{\text{total}} = \sum_{i=1}^M \nu_i \quad (17)$$

which is then determined as the sum over all processes contained in the process list. The actual KMC time step Δt for a given configuration is randomly chosen from a Poisson distribution

$$\Delta t = -\frac{\ln(u)}{\nu_{\text{total}}} \quad (18)$$

where $u \in [0, 1]$ is a uniform random deviate. The time step Δt is independent from the chosen hopping process. To select the actual jump, we define process probabilities according to $p_i = \sum_{j=1}^i \nu_j / \nu_{\text{total}}$. The i th process is chosen, when $p_{i-1} < \nu < p_i$, where $\nu \in [0, 1]$ is another uniform random deviate. After having performed a hop, the process list is updated. In order to avoid wall effects, we employ periodic boundary conditions. We have investigated the finite size effect on the diffusivity and found systems of $5 \times 5 \times 5$ unit cells to be sufficiently large and giving satisfactory results [22]. In order to provide sufficiently accurate data for the Onsager transport coefficient L_{ij} , a total of 10^8 – 10^9 simulation steps were required. These simulations extended to several CPU days on a single IBM SP2 node.

For ternary mixtures, applying linear response theory, the Onsager coefficients L_{ij} can be determined using the displacement formula

$$L_{ij} = \lim_{\Delta t \rightarrow \infty} L_{ij}(\Delta t) = \frac{1}{6} \frac{1}{N_s} \lim_{\Delta t \rightarrow \infty} \frac{1}{\Delta t} \left\langle \left(\sum_{l=1}^{N_i} (\mathbf{r}_{l,i}(t + \Delta t) - \mathbf{r}_{l,i}(t)) \right) \times \left(\sum_{k=1}^{N_j} (\mathbf{r}_{k,j}(t + \Delta t) - \mathbf{r}_{k,j}(t)) \right) \right\rangle \quad (19)$$

where $\langle \dots \rangle$ denotes both ensemble and time averaging over the entire system trajectory, N_i the number of particles belong to species i , $\mathbf{r}_i(t)$ the position vector of component i at time t . In contrast to the formula for L_{ij} used by Sanborn and Snurr [26] in their MD simulations, the normalising volume is replaced by N_s , the total number of discrete adsorption sites in the simulation. Furthermore, Eq. (19) yields the L_{ij} in units of m^2/s . The Onsager coefficients L_{ij} are subject to strong correlation effects and therefore the obtained values

of the transport coefficients vary strongly with the separation time between two configurations Δt ; a Δt of 0.002 s was employed on the basis of our previous experience [22].

4. KMC simulation results compared to the MS model predictions

In the first series of KMC simulations with the ternary mixture, we keep the mixture composition constant and $\theta_1 = \theta_2 = \theta_3 = 0.333$ for each species and study the influence of varying the total occupancy ($\theta_1 + \theta_2 + \theta_3$). The KMC simulation results for the L_{ij} are shown in Fig. 3 as open symbols. The MS model calculations of the main and cross-coefficients using Eqs. (12), (13) and (15) are shown in Fig. 3(a) and (b) as continuous lines. We note that the main coefficients are predicted with excellent accuracy. The off-diagonal elements are also predicted reasonably well. We also performed calculations of the MS model in which the exchange coefficients \mathcal{D}_{ij} are taken to have infinitely large values, corresponding to zero correlations between molecular jumps. With this assumption, the cross-coefficients vanish and the main coefficients L_{ii} correspond to those of the pure components. The comparison of the main coefficients with KMC simulations are shown in Fig. 3(c). We note that the match between simulations and the no correlations model is quite poor, especially for component 3. The reason for this poor match can be explained as follows. Correlation effects tend to slow down the faster moving species. In the system under study, the fastest moving species 3 will be slowed down by both species 1 and 2. The slowest moving species 1 will be speeded up by species 2 and 3. Species 2 is accelerated by species 3, but decelerated by species 2. Clearly, neglect of correlation effects leads to poor predictions of L_{ii} . The main coefficients cannot be identified with the pure component L_s , as has been suggested by Sundaram and Yang [6].

Next, we performed a set of three KMC simulations in which the total occupancy was held constant ($\theta_1 + \theta_2 + \theta_3 = 0.48$) but the mixture compositions were varied. In Fig. 4, we present the simulation results which were carried out for an equimolar mixture of species 2 and 3 in which the mole fraction of component 1 (slowest species), $\theta_1/(\theta_1 + \theta_2 + \theta_3)$ was varied from 0 to 1. The continuous lines in Fig. 4(a) and (b) represent the MS model calculations, using Eqs. (12), (13) and (15), are seen to be in good agreement with the KMC simulation results. Ignoring the correlations (by effectively taking $ij \rightarrow \infty$) leads to much poorer predictions of the main coefficients L_{ii} ; see Fig. 4(c). We also note from Fig. 4(c) that the deviations are particularly large for L_{22} and L_{33} ; this is because the species 2 and 3 are slowed down by species 1 due to correlations. Ignoring correlated jump effects will lead to poor estimations of L_{22} and L_{33} .

In Fig. 5, we present the simulation results which were carried out for an equimolar mixture of species 1 and 3 in which the mole fraction of component 2 (species with

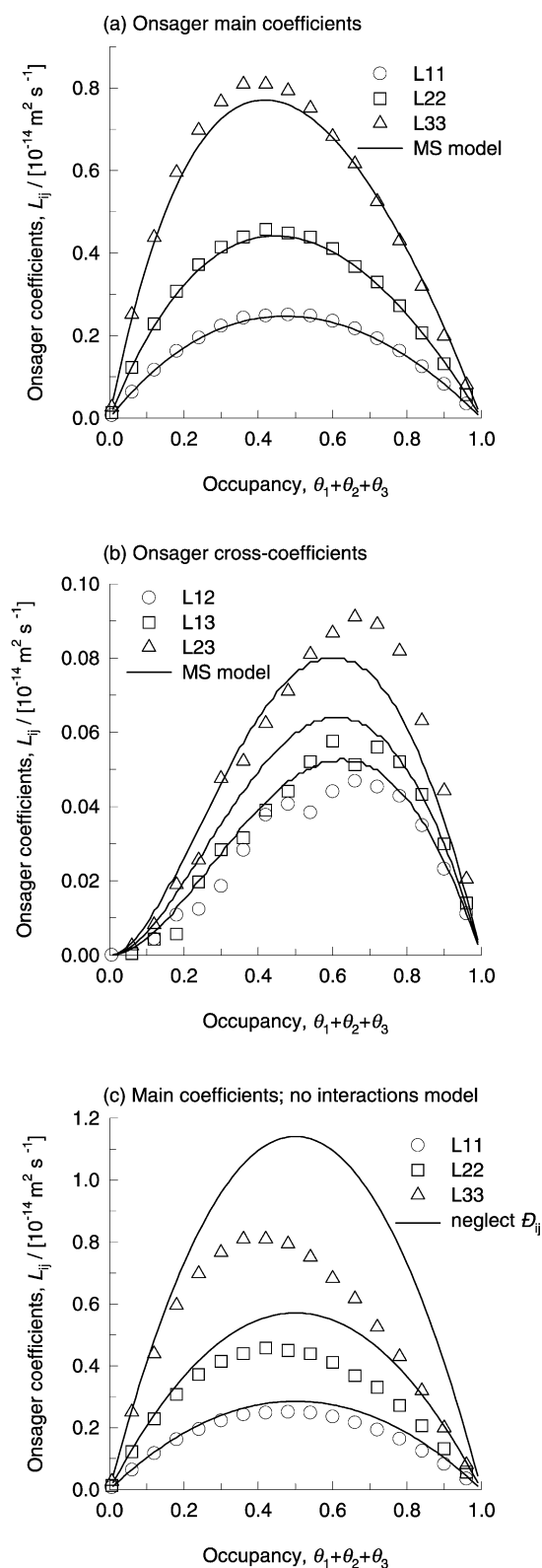


Fig. 3. KMC simulations for L_{ij} in ternary mixture as a function of total occupancy ($\theta_1 + \theta_2 + \theta_3$). In these simulations we keep $\theta_1 = \theta_2 = \theta_3 = 0.333$ for each species. The pure component parameters are specified in Table 1. The KMC simulation results for the L_{ij} are shown as open symbols. The continuous lines in (a) and (b) are obtained using Eqs. (12), (13) and (15).

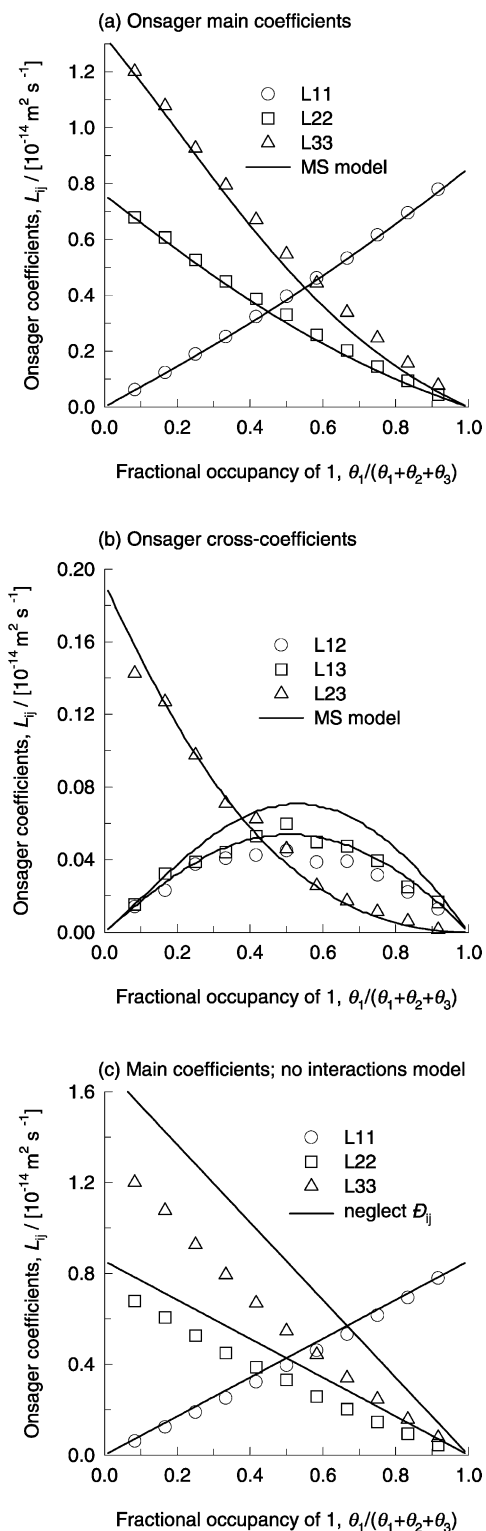


Fig. 4. KMC simulations for L_{ij} in ternary mixture as a function of mole fraction of component 1, $\theta_1/(\theta_1 + \theta_2 + \theta_3)$ with the total occupancy kept constant ($\theta_1 + \theta_2 + \theta_3$) = 0.48. The mixture is equimolar in species 2 and 3. The pure component parameters are specified in Table 1. The KMC simulation results for the L_{ij} are shown as open symbols. The continuous lines in (a) and (b) are obtained using Eqs. (12), (13) and (15). In (c) the continuous lines are the calculations for the main coefficients L_{ii} obtained by making the assumption that the interchange coefficients \mathcal{D}_{ij} have infinite values (no correlations in molecular jumps).

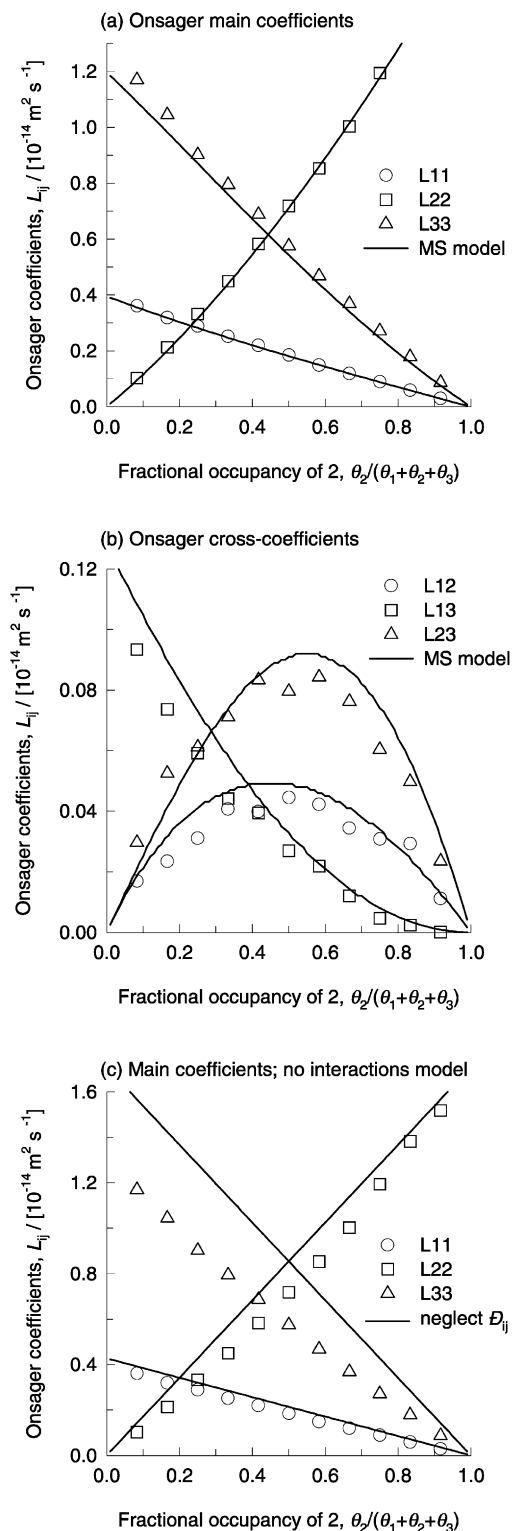


Fig. 5. KMC simulations for L_{ij} in ternary mixture as a function of mole fraction of component 2, $\theta_2/(\theta_1 + \theta_2 + \theta_3)$ with the total occupancy kept constant ($\theta_1 + \theta_2 + \theta_3$) = 0.48. The mixture is equimolar in species 1 and 3. The pure component parameters are specified in Table 1. The KMC simulation results for the L_{ij} are shown as open symbols. The continuous lines in (a) and (b) are obtained using Eqs. (12), (13) and (15). In (c) the continuous lines are the calculations for the main coefficients L_{ii} obtained by making the assumption that the interchange coefficients \mathcal{D}_{ij} have infinite values (no correlations in molecular jumps).

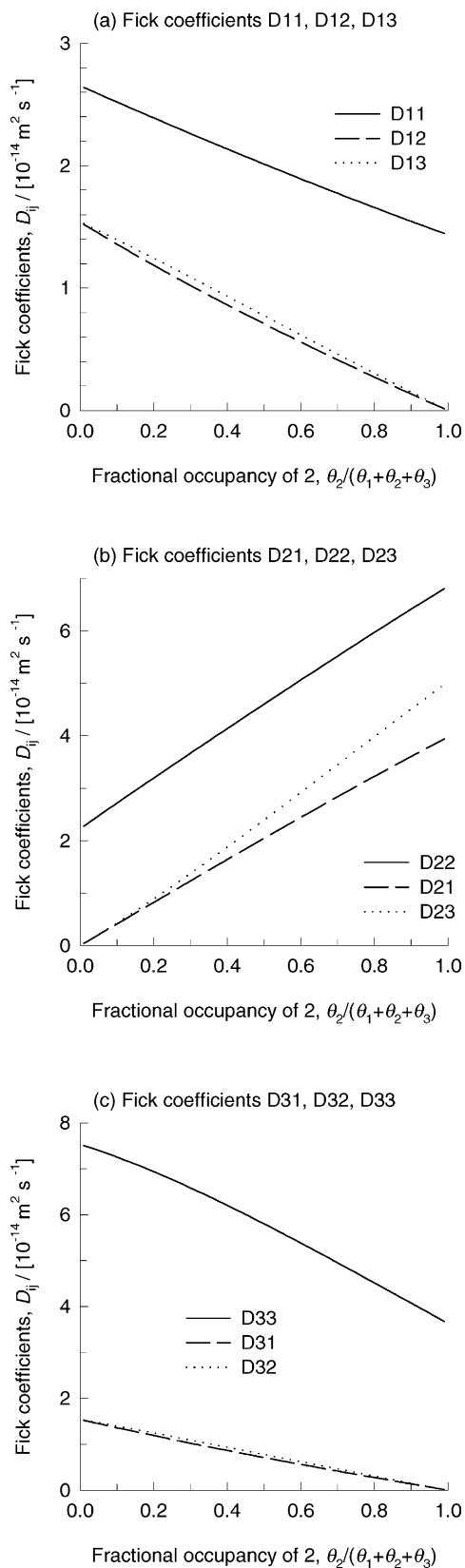


Fig. 6. Calculations of the elements of the Fick matrix $[D]$ in ternary mixture as a function of mole fraction of component 2, $\theta_2/(\theta_1 + \theta_2 + \theta_3)$ with the total occupancy kept constant $(\theta_1 + \theta_2 + \theta_3) = 0.48$. The mixture is equimolar in species 1 and 3.

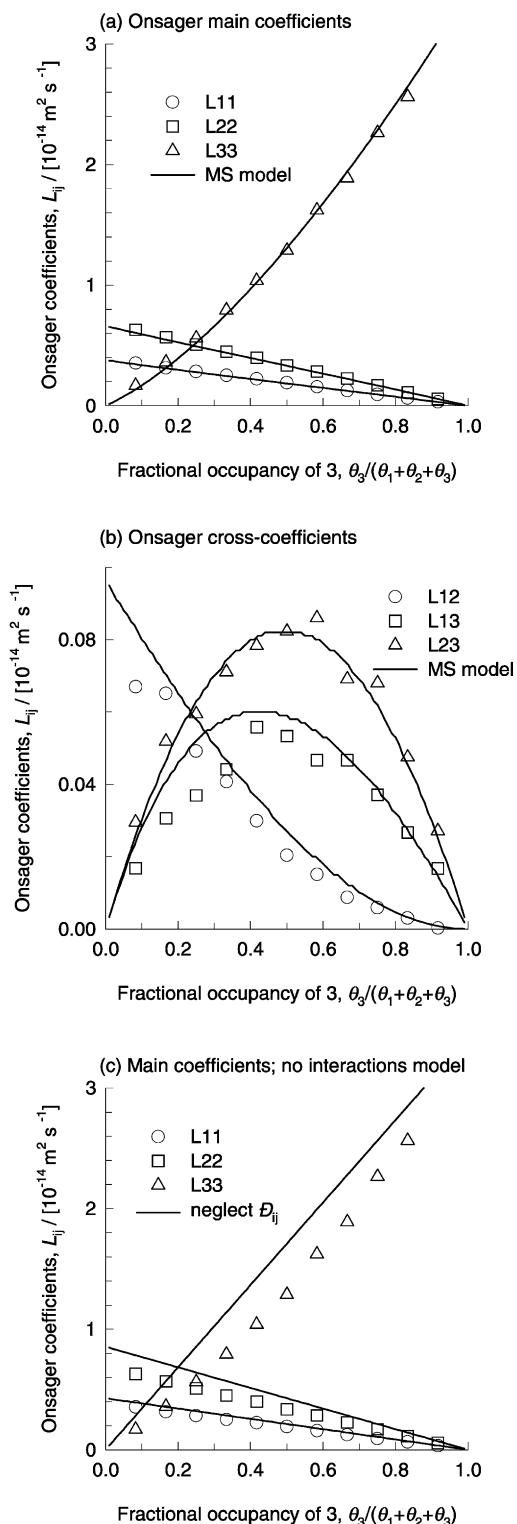


Fig. 7. KMC simulations for L_{ij} in ternary mixture as a function of mole fraction of component 3, $\theta_3/(\theta_1 + \theta_2 + \theta_3)$ with the total occupancy kept constant $(\theta_1 + \theta_2 + \theta_3) = 0.48$. The mixture is equimolar in species 1 and 2. The pure component parameters are specified in Table 1. The KMC simulation results for the L_{ij} are shown as open symbols. The continuous lines in (a) and (b) are obtained using Eqs. (12), (13) and (15). In (c) the continuous lines are the calculations for the main coefficients L_{ij} obtained by making the assumption that the interchange coefficients \mathcal{D}_{ij} have infinite values (no correlations in molecular jumps).

intermediate mobility), $\theta_2/(\theta_1 + \theta_2 + \theta_3)$ was varied from 0 to 1. The continuous lines in Fig. 5(a) and (b) represent the MS model calculations, using Eqs. (12), (13) and (15), are seen to be in good agreement with the KMC simulation results. Ignoring the correlations (by effectively taking $\mathcal{D}_{ij} \rightarrow \infty$) leads to much poorer predictions of the main coefficients L_{ii} ; see Fig. 5(c).

From Eq. (8), we can calculate the nine elements of the Fick matrix $[D]$; these are shown in Fig. 6. We see that the off-diagonal elements are significantly non-zero, pointing to strong coupling effects.

Lastly, in Fig. 7, we present the simulation results which were carried out for an equimolar mixture of species 1 and 2 in which the mole fraction of component 3 (fastest species), $\theta_3/(\theta_1 + \theta_2 + \theta_3)$ was varied from 0 to 1. The continuous lines in Fig. 7(a) and (b) represent the MS model calculations, using Eqs. (12), (13) and (15), are seen to be in good agreement with the KMC simulation results. Ignoring the correlations (by effectively taking $\mathcal{D}_{ij} \rightarrow \infty$), leads to much poorer predictions of the main coefficients L_{ii} ; see Fig. 7(c).

5. Conclusions

We have developed the MS formulation for mixture diffusion in zeolites and compared this with the Onsager formulation. Both approaches have their roots in the theory of IT. An important advantage of the MS formalism is that it allows the estimation of mixture diffusion on the basis of the pure component diffusivities at zero loading. This predictive capability has been tested by carrying out KMC simulations for a ternary mixture in both silicalite. The following major conclusions can be drawn from the results presented in this paper:

- All the six Onsager coefficients L_{ij} are influenced by correlated jump effects. This result is in sharp contrast with the MS diffusivities \mathcal{D}_i which are free of correlation effects [22,23].
- The set of KMC simulation results presented in Figs. 3–5 and 7 validate the predictive capability of the MS formulation. The logarithmic interpolation formula (Eq. (12)) for the interchange coefficients \mathcal{D}_{ij} has been verified.
- Ignoring correlation effects (by effectively taking $\mathcal{D}_{ij} \rightarrow \infty$) leads to much poorer predictions of the main coefficients L_{ii} . Furthermore, ignoring correlations, we predict vanishing cross-coefficients L_{ij} ; this is in sharp contrast with the KMC simulation results which show significant, non-zero values for the cross-coefficients. Our work shows that the procedure suggested by Sundaram and Yang [6] for estimating the main coefficients on the basis of pure component parameters, is not correct.
- From the knowledge of the Onsager matrix $[L]$, the elements of the Fick matrix $[D]$ can be calculated using Eq. (8).

We conclude that the Maxwell–Stefan theory for multicomponent diffusion in zeolites can be used to predict mixture behaviour with good accuracy from pure component transport data.

Acknowledgements

RK and DP acknowledge a grant *Programmasubsidie* from the Netherlands Organisation for Scientific Research (NWO) for the development of novel concepts in reactive separations technology.

References

- [1] J. Kärger, D.M. Ruthven, *Diffusion in Zeolites and other Microporous Solids*, Wiley, New York, 1992.
- [2] D.M. Ruthven, M.F.M. Post, *Diffusion in zeolite molecular sieves*, in: H. van Bekkum, E.M. Flanigan, J.C. Jansen (Eds.), *Introduction to Zeolite Science and Practice*, 2nd Edition, Elsevier, Amsterdam, 2000.
- [3] D.M. Ruthven, *Principles of Adsorption and Adsorption Processes*, Wiley, New York, 1984.
- [4] R. Krishna, J.A. Wesselingh, The Maxwell–Stefan approach to mass transfer, *Chem. Eng. Sci.* 52 (1997) 861–911.
- [5] J. Kärger, Some remarks on the straight and cross-coefficients in irreversible thermodynamics of surface flow and on the relation between diffusion and self diffusion, *Surf. Sci.* 36 (1973) 797–801.
- [6] N. Sundaram, R.T. Yang, Binary diffusion of unequal sized molecules in zeolites, *Chem. Eng. Sci.* 55 (2000) 1747–1754.
- [7] F.J. Keil, R. Krishna, M.O. Coppens, Modeling of diffusion in zeolites, *Rev. Chem. Eng.* 16 (2000) 71–197.
- [8] F. Kapteijn, J.A. Moulijn, R. Krishna, The generalized Maxwell–Stefan model for diffusion in zeolites: sorbate molecules with different saturation loadings, *Chem. Eng. Sci.* 55 (2000) 2923–2930.
- [9] R. Krishna, D. Paschek, Separation of hydrocarbon mixtures using zeolite membranes: a modelling approach combining molecular simulations with the Maxwell–Stefan theory, *Sep. Purif. Technol.* 21 (2000) 111–136.
- [10] D.A. Reed, G. Ehrlich, Surface diffusivity and the time correlation of concentration fluctuations, *Surf. Sci.* 105 (1981) 603–628.
- [11] D.A. Reed, G. Ehrlich, Surface diffusion, atomic jump rates and thermodynamics, *Surf. Sci.* 102 (1981) 588–609.
- [12] L. Riekert, Rates of sorption and diffusion of hydrocarbons in zeolites, *AIChE J.* 17 (1971) 446–454.
- [13] V.P. Zhdanov, General equations for description of surface diffusion in the framework of the lattice gas model, *Surf. Sci.* 194 (1985) L13–L17.
- [14] J. Kärger, Random-walk through 2-channel networks—a simple means to correlate the coefficients of anisotropic diffusion in ZSM-5 type zeolites, *J. Phys. Chem.* 95 (1991) 5558–5560.
- [15] B. Smit, L.D.J.C. Loyens, G.L.M.M. Verbist, Simulation of adsorption and diffusion of hydrocarbons in zeolites, *Faraday Discuss.* 106 (1997) 93–104.
- [16] S. Pal, K.A. Fichthorn, Accelerated molecular dynamics of infrequent events, *Chem. Eng. J.* 74 (1999) 77–83.
- [17] C. Tunca, D.M. Ford, A transition-state theory approach to adsorbate dynamics at arbitrary loadings, *J. Chem. Phys.* 111 (1999) 2751–2760.
- [18] T.J.H. Vlugt, C. Dellago, B. Smit, Diffusion of isobutane in silicalite studied by transition path sampling, *J. Chem. Phys.* 113 (2000) 8791–8799.

- [19] R.L. June, A.T. Bell, D.N. Theodorou, Transition-state studies of Xenon and SF₆ diffusion in silicalite, *J. Phys. Chem.* 95 (1991) 8866–8878.
- [20] D. Paschek, R. Krishna, Monte Carlo simulations of sorption and diffusion of isobutane in silicalite, *Chem. Phys. Lett.* 342 (2001) 148–154.
- [21] D. Paschek, R. Krishna, Diffusion of binary mixtures in zeolites: kinetic Monte Carlo vs. molecular dynamics simulations, *Langmuir* 17 (2001) 247–254.
- [22] D. Paschek, R. Krishna, Monte Carlo simulations of self-and transport-diffusivities of 2-methylhexane in silicalite, *Phys. Chem. Chem. Phys.* 2 (2000) 2389–2394.
- [23] D. Paschek, R. Krishna, Inter-relation between self-and jump-diffusivities in zeolites, *Chem. Phys. Lett.* 333 (2001) 278–284.
- [24] S.M. Auerbach, Theory and simulation of jump dynamics, diffusion and phase equilibrium in nanopores, *Int. Rev. Phys. Chem.* 19 (2000) 155–198.
- [25] M.O. Coppens, A.T. Bell, A.K. Chakraborty, Dynamic Monte-Carlo and mean-field study of the effect of strong adsorption sites on self-diffusion in zeolites, *Chem. Eng. Sci.* 54 (1999) 3455–3463.
- [26] M.J. Sanborn, R.Q. Snurr, Diffusion of binary mixtures of CF₄ and *n*-alkanes in faujasite, *Sep. Purif. Technol.* 20 (2000) 1–13.